Clays and Clay Minerals, Vol. 63, No. 6, 469–484, 2015.

DIAGENETIC AND PALEOENVIRONMENTAL CONTROLS ON LATE CRETACEOUS CLAY MINERALS IN THE SONGLIAO BASIN, NORTHEAST CHINA

YUAN GAO[1], CHENGSHAN WANG[1,*], ZHIFEI LIU[2], XIAOJING DU[3], AND DANIEL E. IBARRA[4]

[1] State Key Laboratory of Biogeology and Environmental Geology, School of Earth Sciences and Resources, China University of Geosciences (Beijing), Beijing 100083, China
[2] State Key Laboratory of Marine Geology, Tongji University, Shanghai 200092, China
[3] Department of Earth and Environmental Sciences, University of Michigan, Ann Arbor, Michigan 48109, USA
[4] Department of Earth System Science, Stanford University, Stanford, California 94305-4216, USA

Abstract—Sedimentary and diagenetic processes control the distribution of clay minerals in sedimentary basins, although these processes have seldom been studied continuously in continental sedimentary basins. The Songliao Basin, northeast China, is a large continental, petroleum-bearing basin, and provides a unique study site to understand the sedimentary and diagenetic processes that influence clay assemblages. In this paper, the clay mineralogy of a 2500 m-thick Late Cretaceous (late Turonian to Maastrichtian) terrestrial sedimentary succession (SK-1s and SK-1n cores), retrieved by the International Continental Scientific Drilling Program in the Songliao Basin, was examined. The objective was to determine the diagenetic and paleoenvironmental variations that controlled the formation of clay mineral assemblages, and to determine the thermal and paleoenvironmental evolution of the basin. The results from both cores show that illite is ubiquitous through the succession, smectite is frequently encountered in the upper strata, and ordered mixed-layer illite-smectite (I-S), chlorite, and kaolinite are abundant in the lower strata. Burial diagenesis is the primary control on the observed decrease of smectite and increasing illite, I-S, and chlorite with depth. Observations of clay-mineral diagenesis are used to reconstruct the paleotemperatures and maximum burial depths to which the sediments were subjected. The lowermost sediments could have reached a maximum burial of ~1000 m deeper than today and temperatures ~50ºC higher than today in the latest Cretaceous. The transition of smectite to I-S in the SK-1 cores and the inferred paleotemperatures provide new constraints for basin modeling of oil maturation at elevated temperatures in the Songliao Basin. Authigenic kaolinite and smectite are enriched in sandstones with respect to the coeval mudstones from the SK-1n core, as a result of early diagenesis with the participation of primary aluminosilicates and pore fluids. In the upper part of both SK-1 cores, variations in smectite and illite were controlled primarily by paleoenvironmental changes. Increases in smectite and decreases in illite from the late Campanian to Maastrichtian are interpreted as resulting from increasing humidity, a conclusion consistent with previous paleoenvironmental interpretations.

Key Words—Clay Minerals, Diagenesis, Thermal Evolution, Paleoenvironment, Late Cretaceous, Songliao Basin, China.

INTRODUCTION

Clay minerals (<2 μm phyllosilicates) in sedimentary basins are controlled by multiple factors during sedimentary and diagenetic processes (Chamley, 1989; Thiry, 2000; Środoń *et al.*, 2013). Sedimentary clay minerals are weathering products of rocks in the source area, which are influenced by provenance lithology, paleoclimate, depositional environment, *etc.* (*e.g.* Chamley, 1989). These clay minerals may originate from physical weathering on parent rocks, from leaching and reorganization of ions under climatic conditions with more intense chemical weathering, or from differential sorting and settling during transportation and deposition (Singer, 1984; Thiry, 2000). Using semi-quantitative identification methods, clay minerals controlled by sedimentary processes have been used successfully to reconstruct paleoenvironments in a variety of sedimentary basins of various ages (Sáez *et al.*, 2003; Deconinck *et al.*, 2005; Dera *et al.*, 2009; Liu *et al.*, 2010).

Diagenetic processes, driven by either post-depositional changes in pore-water chemistry or by increasing temperature with increased sedimentary burial, can significantly change the primary clay composition (Hower *et al.*, 1976; Chamley, 1989; Środoń, 1999; Bjørlykke, 2014). In shallow-buried sediments, early diagenesis is characterized by authigenesis of secondary clay minerals during interaction of primary aluminosilicates and pore fluids (Wilson and Pittman, 1977; Vanderaveroet and Deconinck, 1997; Bjørlykke, 2014). For example, authigenic kaolinite may precipitate under low K^+/H^+ and low silica concentrations in the pore water, which can be derived from meteoric water or organic acids (Bjørlykke, 1998; Wilson *et al.*, 2014). Precipitation of smectite is induced by the presence of volcanic substrates under various conditions (Cuadros *et al.*, 1999; Fesharaki *et al.*, 2007). Early diagenesis, therefore, not only undermines the use of clay-mineral

* E-mail address of corresponding author:
chshwang@cugb.edu.cn
DOI: 10.1346/CCMN.2015.0630605

assemblages for paleoenvironmental reconstruction, but also causes formation damage to reservoir sandstone in petroleum-bearing sedimentary basins (Bjørlykke, 2014; Wilson *et al.*, 2014).

Burial diagenesis changes the clay mineralogical assemblages in deeper buried sediments by a series of governing chemical reactions, including the smectite–illite transformation, kaolinite–illite transformation, *etc.* (Hower *et al.*, 1976; Środoń, 1999; Day-Stirrat *et al.*, 2010). Although variables such as reaction order and inorganic fluid chemistry may influence these clay mineralogical changes (Pytte and Reynolds, 1988; Velde and Vasseur, 1992; Huang *et al.*, 1993; Elliott and Matisoff, 1996; Środoń, 1999), the most important factor is increasing temperature during burial (Hower *et al.*, 1976; Środoń, 1999; Osborn *et al.*, 2014). Clay minerals formed during burial diagenesis have been used to estimate the thermal and tectonic evolution of sedimentary rocks in basins and mountain belts (Bjørlykke, 1998; Wilkinson *et al.*, 2006; Deconinck *et al.*, 2014).

Analyses of sedimentary and diagenetic processes controlling clay mineral assemblages have been carried out primarily in marine sedimentary basins (*e.g.* Hower *et al.*, 1976; Bjørlykke, 1998; Day-Stirrat *et al.*, 2010). In continental sedimentary basins, however, these processes have seldom been studied continuously, due to the fragmentary and discontinuous nature of terrestrial sedimentation. The Songliao Basin in northeastern China, which is a large and long-lived, Cretaceous, continental sedimentary basin, provides a suitable site to study different controls on clay-mineral assemblages in terrestrial sediments. This basin preserves a terrigenous sequence up to 10,000 m thick and contains a rich petroleum reservoir: >40 billion barrels of proven oil reserves and >300 billion m^3 of proven natural gas reserves (Hou *et al.*, 2009; Feng *et al.*, 2010; Wang *et al.*, 2013a). The thick and nearly continuous terrigenous sequence in the Songliao Basin provides an opportunity for terrestrial paleoclimatic studies of the Cretaceous climatic optimum (Wang *et al.*, 2013a, 2013b). Many paleoenvironmental proxies, including clay minerals, have been applied previously to outcrop and core sediments over the past two decades (Wang *et al.*, 1994; Gao *et al.*, 1999; Gao *et al.*, 2013; Wang *et al.*, 2013a). Researchers have been cautious about interpreting whether these proxies were altered by diagenesis (Wang, G. *et al.*, 2008; Chamberlain *et al.*, 2013), and a systematic study of clay mineralogy may provide evidence for the diagenetic processes influencing these sediments. On the other hand, diagenetic clay minerals may provide information about the thermal evolution of sedimentary rocks, although they have been applied minimally in previous sedimentology and petroleum geology studies of the Songliao Basin (Wang *et al.*, 1990; Sun *et al.*, 2007; Gao *et al.*, 2013).

The present study takes advantage of the >2500 m of nearly continuous, terrestrial sediments of Cretaceous age obtained by the first phase of the Continental Scientific Drilling Project of Cretaceous Songliao Basin (SK-1), which is the only drilling project targeting Cretaceous terrestrial strata under the framework of the International Continental Scientific Drilling Program (ICDP). The clay mineralogy of the SK-1 cores was examined at a detailed sampling interval (~10 m) through the Late Cretaceous. The objectives of the present study were: (1) to determine the diagenetic and sedimentary origins of the clay minerals; (2) to discuss the implications of diagenetic clay minerals for the thermal and tectonic evolution of the Songliao Basin; and (3) to interpret the terrestrial paleoenvironment of the Songliao Basin in the Late Cretaceous based on sedimentary clay minerals when they can be proved as being minimally influenced by diagenesis.

GEOLOGICAL SETTING

The Songliao Basin is 750 km long, 330–370 km wide, and covers roughly 260,000 km^2 in northeastern China (Figure 1; Wang *et al.*, 2013a). Up to 10,000 m of volcaniclastic, alluvial fan, fluvial, and lacustrine sediments were deposited during the basin evolution in Cretaceous times (Chen and Chang, 1994; Wang *et al.*, 1994; Feng *et al.*, 2010). The 'Continental Scientific Drilling project of Cretaceous Songliao Basin,' under the ICDP framework, is currently underway, designed to obtain a continuous terrestrial Cretaceous record which is as complete as possible (Feng *et al.*, 2013; Wang *et al.*, 2013a). In its first phase (namely the SK-1 drilling project) completed in 2007, ~2500 m of core of Late Cretaceous age was recovered with a recovery ratio of ~95% (Wang, C.S. *et al.*, 2008; Feng *et al.*, 2013). An ongoing second phase (SK-2 drilling project) has the goal of coring the Lower Cretaceous and Upper Jurassic terrestrial strata in the Songliao Basin (Wang, C.S. *et al.*, 2008; Feng *et al.*, 2013).

The SK-1 drilling project consisted of two boreholes, the south borehole (SK-1s) and the north borehole (SK-1n), which are 60 km apart (Figures 1, 2). Six stratigraphic formations in both cores have been identified and a basin-wide oilshale layer near the base of the Nenjiang Formation (Fm.) has been used to correlate the two cores (Figures 2, 3; Feng *et al.*, 2013). Based upon a combination of biostratigraphy, magnetostratigraphy, cyclostratigraphy, and radiometric datings, the age of the cores has been constrained from late Turonian in the Quantou Fm. to the end-Cretaceous in the Mingshui Fm. (Figure 3; Li *et al.*, 2011; He *et al.*, 2012; Scott *et al.*, 2012; Deng *et al.*, 2013; Wan *et al.*, 2013; Wu *et al.*, 2013, 2015).

Tectonic evolution of the Songliao Basin

During the Late Mesozoic, an extensional rift-valley system developed in northeastern China and southern Mongolia which may have resulted from the interaction

https://doi.org/10.1346/CCMN.2015.0630605 Published online by Cambridge University Press

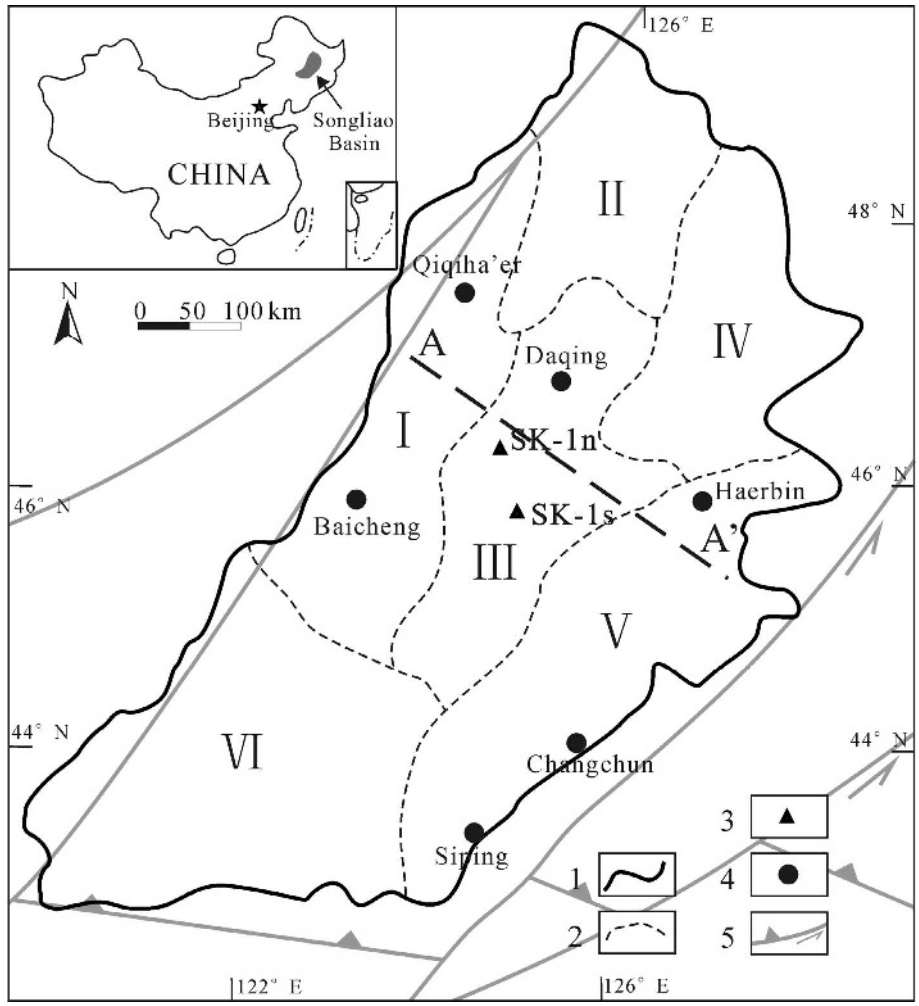

Figure 1. Major structural zones in the Songliao Basin and the drilling sites of SK-1s and SK-1n. (I) Western Slope Zone; (II) Northern Plunge Zone; (III) Central Downwarp Zone; (IV) Northeastern Uplift Zone; (V) Southeastern Uplift Zone; (VI) Southwestern Uplift Zone. (1) Basin Boundary; (2) First-order structural boundary; (3) Drilling sites of SK-1 (north borehole – SK-1n and south borehole – SK-1s); (4) cities; (5) faults. A–A′ and the dashed line indicate the location of the structure cross-section in Figure 2 (modified after Feng *et al.* (2013) and Wang *et al.* (2013b)).

between the Eurasian and Pacific plates (Graham *et al.*, 2001; Ren *et al.*, 2002). The Songliao Basin in northeastern China was formed as a rift basin in this extensional system from the Late Jurassic through the Cretaceous (Graham *et al.*, 2001; Ren *et al.*, 2002; Feng *et al.*, 2010).

Four episodes of deformation, which are related to regional tectonics and associated with stratigraphic signatures, are recognized in the Songliao Basin: mantle upwelling, rifting, post-rift thermal subsidence, and structural inversion (Feng *et al.*, 2010). The episodes of mantle upwelling and rifting occurred from the Middle Jurassic to the Early Cretaceous and formed thick volcanic strata and alluvial and fluvial strata not cored by SK-1 (Feng *et al.*, 2010, 2013).

During post-rift thermal subsidence, regional deformation and subsidence were caused by lithospheric cooling and extension from the Early Cretaceous to the Late Cretaceous (Feng *et al.*, 2010). The Songliao Basin gradually evolved to a large lake with lake-level fluctuations and possible marine incursions (Wang *et al.*, 1994; Wang *et al.*, 2013b). Typical sediment packages are 3000–4000 m thick, with a maximum thickness of 6000 m, comprising lacustrine, fluvial, and alluvial sediments (Wang *et al.*, 2013a). Sediments in the SK-1 cores were mostly deposited during the post-rift thermal subsidence stage.

Structural inversion, including uplift and folding due to subduction of the Pacific plate, began with deposition of the upper Nenjiang Fm. and culminated at the end of the Cretaceous (Feng *et al.*, 2010). The eastern part of the basin underwent continuous uplift (northeastern and southeastern uplift zones shown in Figure 1), causing westward migration of the depocenter and the absence of

https://doi.org/10.1346/CCMN.2015.0630605 Published online by Cambridge University Press

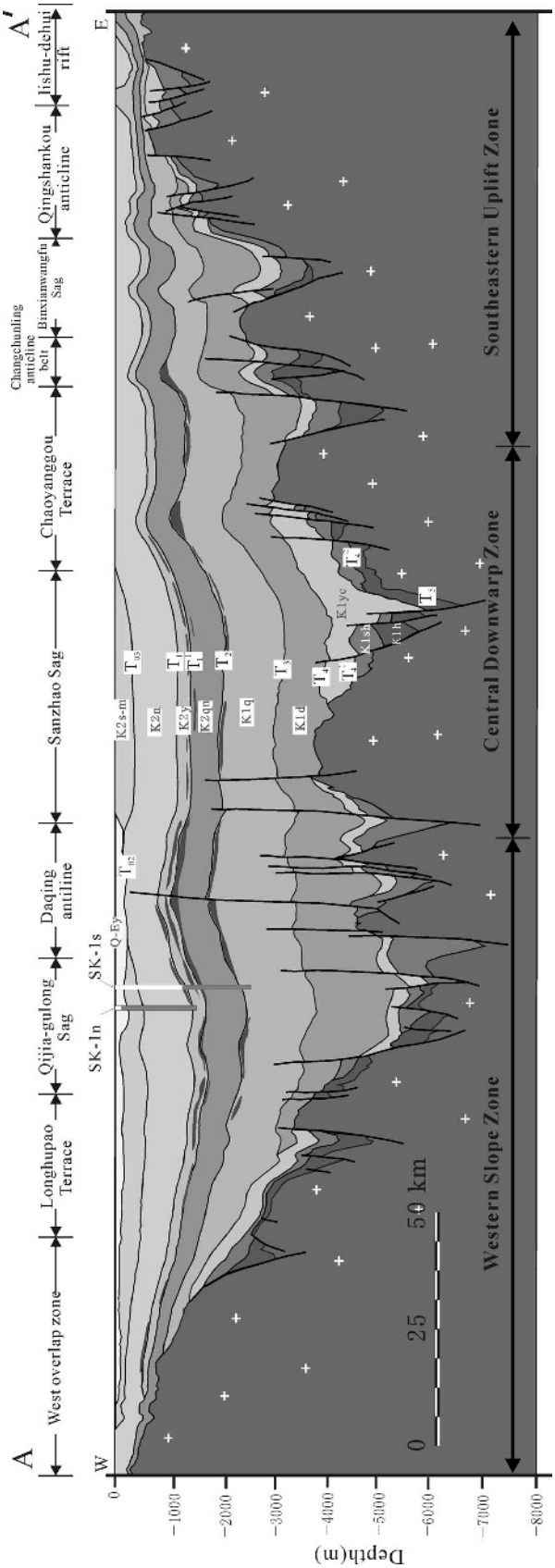

Figure 2. Structural cross-section across the central part of the Songliao Basin based on regional seismic analyses. Lithologies and formations are derived from geophysical logs and cores tied to seismic sections. Q-Ey, Quaternary/Neogene; K2s-m, Sifangtai Fm. and Mingshui Fm.; K2n, Nenjiang Fm.; K2y, Yaojia Fm.; K2qn, Qingshankou Fm.; K1q, Quantou Fm.; K1d, Dengloulou Fm.; K1yc,Yingcheng Fm.; K1sh, Shahezi Fm.; K1h, Houshigou Fm. T03—5, seismic horizons. The gray bars in SK-1n and SK-1s are coring intervals and the white bars are uncored intervals (modified after Wang *et al.*, 2013a).

https://doi.org/10.1346/CCMN.2015.0630605 Published online by Cambridge University Press

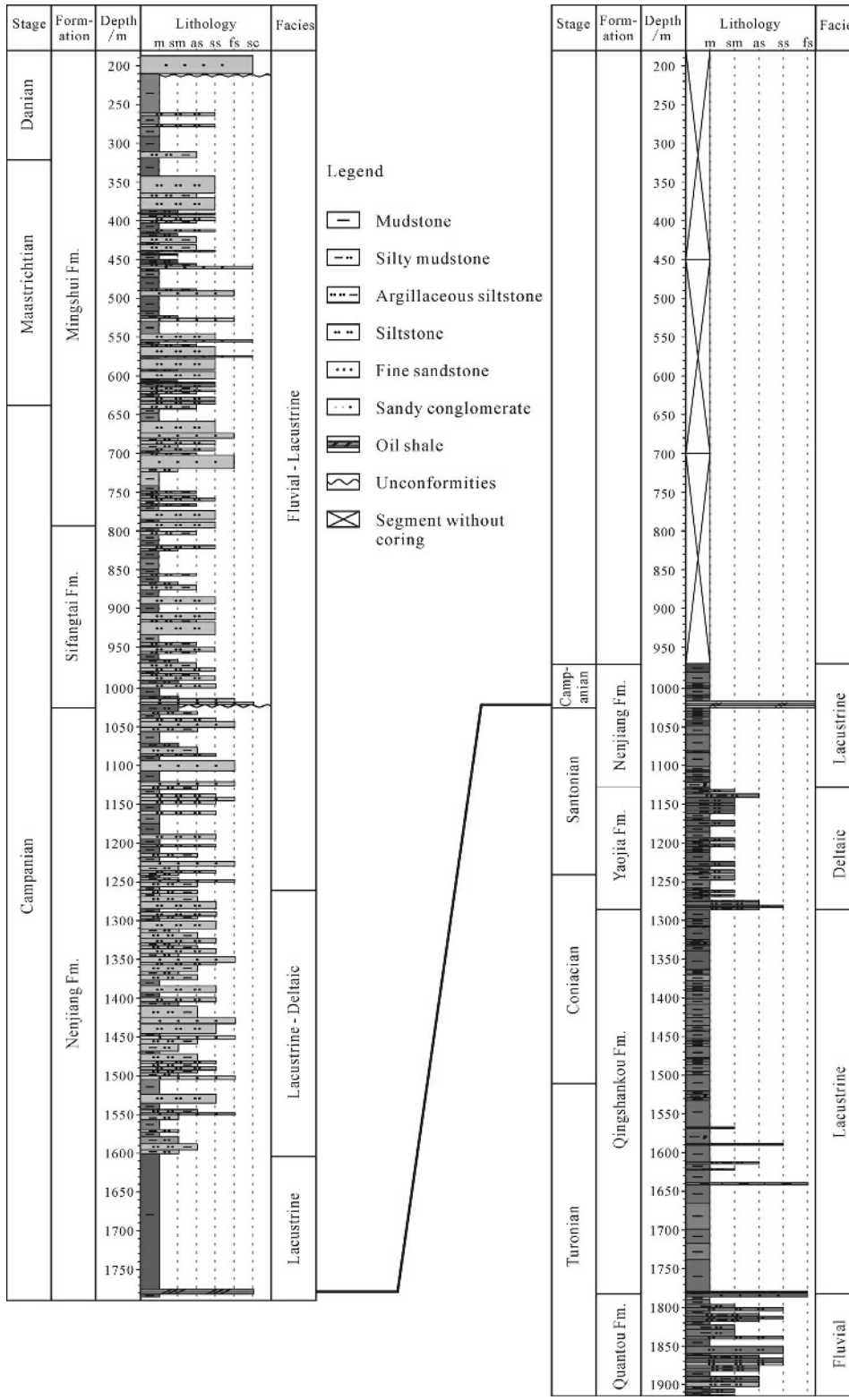

Figure 3. Stratigraphic logs of the SK-1n (left) and SK-1s (right) cores. The two core sections can be correlated by the basin-wide oil shale layer at the lower part of Nenjiang Fm. The differences in the grayscales in the figure indicate the different colors of the rock. Abbreviations: m – mudstone; sm – silty mudstone; as – argillaceous siltstone; ss – siltstone; fs – fine sandstone; sc – sandy conglomerate. Note that the scale of the oil shale marker beds is exaggerated (modified after Feng *et al.* (2013) and Wan *et al.* (2013)).

https://doi.org/10.1346/CCMN.2015.0630605 Published online by Cambridge University Press

Sifangtai-Mingshui Formations on the eastern side of the basin (Xiang *et al.*, 2007; Chen *et al.*, 2010). During the structural inversion, several regional unconformities developed, most notably on top of the Nenjiang Fm. and on top of the Mingshui Fm. (Chen *et al.*, 2010; Feng *et al.*, 2010). After this stage, six structural units were formed in the Songliao Basin: the northern plunge, the central downwarp, the northeastern uplift, the southeastern uplift, the southwestern uplift, and the western slope (Figure 1).

Stratigraphic features of the SK-1 cores

The six stratigraphic formations seen in the SK-1 cores consist mainly of mudstones, siltstones, and sandstones, deposited in diverse paleoenvironments ranging from deep lakes to flood plains (Wang *et al.*, 2013a). Sedimentary features of these formations are described below beginning with the base of the section.

The Quantou Fm. (1915 m−1783 m in SK-1s) is the lowermost formation in SK-1 cores; only the upper strata were penetrated by SK-1s. This formation is characterized by interlayered brownish mudstone and grayish sandstone formed in a fluvial environment. The Quantou Fm. is late Turonian in age (Wan *et al.*, 2013).

The Qingshankou Fm. (1783 m−1286 m in SK-1s) consists mainly of black-gray mudstone interbedded with oil shale and gray sandstone and siltstone. The black mudstone in the lower strata of this formation, the most important petroleum source rock in the Songliao Basin, was deposited in a deep lacustrine environment (Feng *et al.*, 2010). The black-gray mudstone in the upper part was formed primarily in a shallow lacustrine environment. The Qingshankou Fm. is late Turonian to late Coniacian in age.

The Yaojia Fm. (1286 m−1128 m in SK-1s) overlies unconformably the Qingshankou Fm. and is represented by deltaic to shallow-lacustrine mudstones and sandstones. The Yaojia Fm. is late Coniacian to early Santonian in age.

The Nenjiang Fm. (1128 m−968 m in SK-1s and 1783 m−1022 m in SK-1n) consists of very different lithologies and depositional environments between its lower and upper units. The lower part consists of deep lacustrine gray to black mudstone, marl, shelly limestone, and oil shale interbedded with gray siltstone and fine sandstone, while the upper part consists of shallow lacustrine to deltaic grayish siltstone, sandstone, and grayish, greenish to brownish mudstone. The Nenjiang Fm. is late Santonian to early Campanian in age.

The Sifangtai Fm. and Mingshui Fm. (1022 m−210 m in SK-1n) are the uppermost two formations in the Cretaceous SK-1 cores. Strata in these two formations are gray-green and brown-red mudstone and sandstone, which comprise sequences of alluvial plain-shore to shallow-lake deposits (Wang *et al.*, 2013). These two formations are late Campanian to Maastrichtian in age. Two large unconformities separate these two formations from the underlying Nenjiang Fm. and overlying Cenozoic strata (Figure 3).

METHODS

X-ray diffraction (XRD) analysis

A total of 276 mudstone and sandstone samples, covering the whole succession and diverse facies, were collected continuously at a ~10 m sampling interval along both SK-1 cores. Sample pretreatments and clay-mineral analysis followed the methods of Gao *et al.* (2013). Samples were ground lightly and then reacted with 0.1 N HCl to remove carbonates. Deflocculation was accomplished by successive washings with distilled water, and particles of <2 μm size were separated by sedimentation and centrifugation (Liu *et al.*, 2004). Clay minerals (<2 μm) were studied using XRD on mounts of non-calcareous clay-sized particles oriented on glass slides. The XRD was carried out using a PANalytical X'Pert PRO diffractometer (Almelo, Netherlands) with CuKα radiation, Ni filter, and divergence slit of 0.38 mm, under 40 kV voltage and 25 mA current, at the State Key Laboratory of Marine Geology, Tongji University, China. Three XRD runs were performed, following air drying, ethylene-glycol solvation for 24 h, and heating at 490ºC for 2 h. The goniometer scan was from 3 to 30º2θ for each run, with a scanning step size of 0.0167º/s.

Identification of clay minerals was by means of the positions of the (001) basal reflections on the XRD patterns under three different conditions (Moore and Reynolds, 1997). In the present study, smectite includes randomly ordered mixed-layer illite-smectite (R = 0, 10−50% illite), with a diagnostic expanded 17 Å peak upon ethylene-glycol treatment, while ordered illite-smectite (R ⩾ 1, >50% illite) is represented as I-S.

Semi-quantitative calculations were carried out on the XRD patterns, collected under ethylene glycol-solution conditions, using the *MacDiff* software (Petschick *et al.*, 1996). The relative abundances of each clay-mineral species were estimated mainly according to the areas of the (001) series of basal reflections, *i.e.* smectites (17 Å), I-S (11−13 Å), illite (10 Å), and kaolinite/chlorite (7 Å). The percentage of smectitic layers in I-S was determined by the locations of smectite-illite 002/001 and 003/002 peaks and the peak around d = 11.1 Å which contains components of the illite 001 reflection and of the fourth order of a 47.0 Å superstructure peak. Relative proportions of kaolinite and chlorite were determined using the ratios of the 3.57/3.54 Å peak areas (Liu *et al.*, 2004).

Scanning electron microscope (SEM) analysis

Based on clay mineralogical composition and sedimentary facies, six samples were selected for SEM analysis at China University of Geosciences (Beijing). Thin sections of the samples were coated with Pt and adhered to the sample tray using Cu. The analysis was

https://doi.org/10.1346/CCMN.2015.0630605 Published online by Cambridge University Press

carried out on thin sections using a Supra 55 Field Emission Scanning Electron Microscopy (FESEM), manufactured by Zeiss (Oberkochen, Germany), in secondary electron imaging mode, with an accelerating voltage of 15 kV, a beam current of 1–3 nA, system vacuum of 5×10^{-5} mbar, a gun vacuum of 2×10^{-9} mbar, and a spot size of 1 μm. Elemental concentrations were determined using an X-act Energy Dispersive X-ray Spectroscopy (EDS) instrument, manufactured by Oxford Instruments (Abingdon, Oxfordshire, England). The relative abundances of the following elements were used to aid in identifying clay minerals: (1) kaolinite – Al; (2) illite – K; (3) chlorite – Fe and/or Mg; (4) smectite – Mg, Ca, and Na.

RESULTS

Clay mineralogy in SK-1n

Illite and smectite are the dominant clay minerals throughout the SK-1n core in which I-S, kaolinite, and chlorite are more abundant in the lower strata. Clay mineral assemblages in SK-1n (Figure 4) show changes with depth and variations between mudstones (black bars) and sandstones (gray bars). Three intervals were identified according to their dominant clay assemblages.

Interval N1, 250 m–820 m in SK-1n (Uppermost Sifangtai Fm. to Mingshui Fm., late Campanian to Maastrichtian). Smectite is dominant; illite, kaolinite, and chlorite are present in minor amounts except for a few samples; and I-S is negligible. In sandstone samples, smectite is very abundant (>80%) in almost all samples (Figure 4), and shows a very intense (001) reflection in XRD patterns (Figure 5a). The XRD reflection of smectite in mudstone samples is less intense compared with those in coeval sandstone samples (Figure 5b).

Interval N2, 820 m–1200 m in SK-1n (Upper Nenjiang Fm. to Sifangtai Fm., mid–late Campanian). Illite and smectite occur as dominant species. Kaolinite and chlorite are present in minor amounts except for a few data points, and I-S is negligible. As in the previous 250 m–820 m interval, smectite is very abundant (>80%) in almost all sandstone samples (Figure 4), and shows a very intense (001) reflection in XRD patterns (Figure 5a). In mudstone samples, the clay composition is dominated by either smectite or illite (Figure 4). The XRD reflections of smectite and illite in mudstone samples are less intense compared with those in sandstone samples (Figure 5b).

Interval N3, 1200 m–1750 m in SK-1n (mid-Nenjiang Fm., mid-Campanian). Less smectite but more illite than the 250 m–1200 m interval was identified, and I-S occurs sparsely in mudstone samples (Figure 4). Kaolinite and chlorite are more abundant, especially in sandstone samples at depths between 1300 m and 1600 m, with sharp kaolinite peaks at 7 Å and for chlorite at 7 Å and 4.72 Å in the XRD patterns (Figure 5c).

Clay mineralogy in SK-1s

The main clay minerals in the SK-1s core are illite, I-S, smectite, and chlorite. Changes in clay mineral assemblages are obvious with depth but not with lithology. Based on clay-mineral assemblage variations, SK-1s was divided into three intervals (Figure 6).

Interval S1, 960 m–1020 m in SK-1s (Lower Nenjiang Fm., early Campanian). Smectite and illite are the predominant clay species (Figure 6). An obvious 17 Å (001) reflection can be identified in the XRD patterns of most samples under EG conditions (Figure 7a). In addition, I-S is absent, kaolinite is negligible, and chlorite is present in most samples, with an average of 7%.

Interval S2, 1020 m–1100 m in SK-1s (Lower Nenjiang Fm., late Santonian). Compared with the previous 960 m–1020 m interval, smectite decreases in abundance with depth while illite increases and becomes dominant (Figure 6). I-S, kaolinite, and chlorite are still minor components.

Interval S3, 1100 m–1915 m in SK-1s (Quantou Fm. to lowermost Nenjiang Fm., late Turonian to early Santonian). Smectite is not present in this interval, illite is the dominant clay mineral, and I-S (average 19% abundance) and chlorite (average 14% abundance) are also common (Figure 6). Based on the low-angle positions of I-S reflections in XRD analysis, the percentages of smectitic layers in I-S are estimated to be 20% at 1915 m and 25% at 1500 m (Figure 7c,d).

Scanning electron microscopy of clay minerals in SK-1

Clay minerals in both SK-1 cores present various morphologies. Previous studies reported that in the sandstones of the upper part of the SK-1n core, smectite formed clay coatings around detrital grains (Fu *et al.*, 2012; Gao *et al.*, 2013). This was confirmed by the present study where smectite coatings with rose-like and honeycomb textures were observed (Figure 8a). In mudstones, however, smectite and illite form plates (Figure 8b). Kaolinite aggregates formed stacked plates in sandstones of the lower part of the SK-1n core (Figure 8c), while individual kaolinite plates present pseudohexagonal outlines (Figure 8d).

DISCUSSION

Burial diagenesis of clay minerals

A series of mineralogical reactions takes place in sediments during burial diagenesis (*e.g.* Hower *et al.*, 1976; Chamley, 1989; Środoń, 1999; Day-Stirrat *et al.*, 2010). Transformations from smectite to illite and chlorite involving mixed-layer clays are the most

https://doi.org/10.1346/CCMN.2015.0630605 Published online by Cambridge University Press

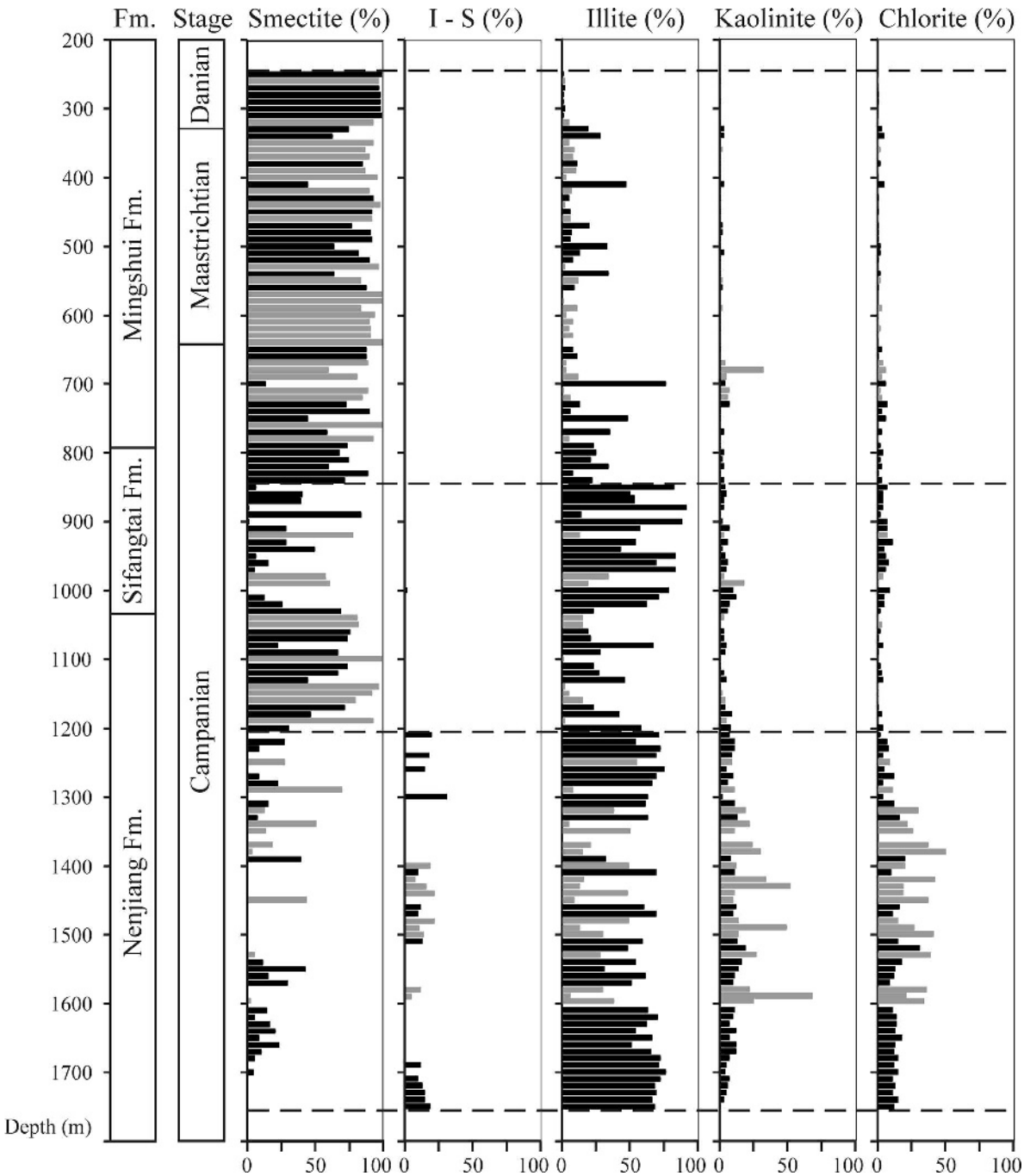

Figure 4. Clay-mineral distribution in the SK-1n core based on XRD results. Black bars – mudstone samples; gray bars – sandstone samples. Dashed lines separate the intervals with different clay assemblages as described in the text.

common burial diagenesis reactions, resulting in greater abundances of illitic and chloritic minerals in more deeply buried sediments (Środoń, 1999; Deconinck *et al.*, 2000).

The clay mineral assemblages in both SK-1 cores show a downward trend of decreasing smectite and increasing illite, I-S, and chlorite (Figures 4, 6). In SK-1s, significant clay mineralogical change occurs at a depth of ~1100 m (Figure 4). Smectite is present above 1100 m and is even dominant above 1023 m. In contrast, below 1100 m, smectite is not present and illite, I-S, and chlorite become dominant. In SK-1n, depth-dependent variations of clay minerals are not as clear as in SK-1s, due to the shallower burial depths, but the general trend

https://doi.org/10.1346/CCMN.2015.0630605 Published online by Cambridge University Press

of decreasing smectite and increasing I-S and chlorite is still observed below a depth of ~1000 m (Figure 6).

The trend of decreasing smectite and increasing illite, I-S, and chlorite with depth in both cores was probably caused by burial diagenesis. According to previous basin-scale studies on clay mineralogy, the precursor clay minerals in the Late Cretaceous sediments in Songliao Basin were considered to have been dominated by illite which originated from weathering of crystalline igneous rocks and smectite which formed from the alteration of volcanic rocks surrounding the basin (Liu, 1985; Wang *et al.*, 1990; Gao *et al.*, 2013). Illite typically persists during burial diagenesis, but smectite tends to incorporate Al^{3+} and K^{+} and form illitic layers, associated with release of Si, Mg, and Fe (Hower *et al.*, 1976; Środoń *et al.*, 1999). Such transformation requires Al and K sourced from the dissolution of adjacent feldspars and mica (Hower *et al.*, 1976; Środoń *et al.*, 1999), and accompanied by the formation of authigenic quartz due to release of silicon (Peltonen *et al.*, 2007). Meanwhile, chlorite is formed in the presence of additional Mg and Fe which are released during the transformation of smectite to illite (Hower *et al.*, 1976; Środoń, 1999), and/or from decomposition of mafic volcanic clasts, commonly found in Songliao Basin sediments (Wang *et al.*, 1994).

Temperature appears to be the primary control on mineralogical reactions during burial diagenesis, especially for the conversion from smectite to illite in shales (Hower *et al.*, 1976; Środoń, 1999; Osborn *et al.*, 2014). Previous studies indicated that for Tertiary and Late Mesozoic basins, the onset of illitization started at 60ºC, the random/ordered mixed layer (R0/R1) transition occurred at ~100ºC (over a range of 75–120ºC), and the long-range ordering (R3) and illite appeared at 165ºC and 210ºC, respectively (Środoń, 1999; Deconinck *et al.*, 2014; Do Campo *et al.*, 2014). The mineralogical changes in diagenesis may allow the thermal history of the deeply buried sediments to be quantified directly. The proportion of smectite in I-S in shales has also been used as a paleogeothermometer, such that 10%, 20%, and 25% smectite (of the total I-S) correspond to isotherms for 180–185ºC, 137–142ºC, and 122–127ºC, respectively (Środoń *et al.*, 2009).

About 20% of the smectite in I-S was estimated for the mudstone at 1915 m depth in SK-1s, based on the low-angle positions of I-S under EG conditions (Figure 7; Moore and Reynolds, 1997; Deconinck *et*

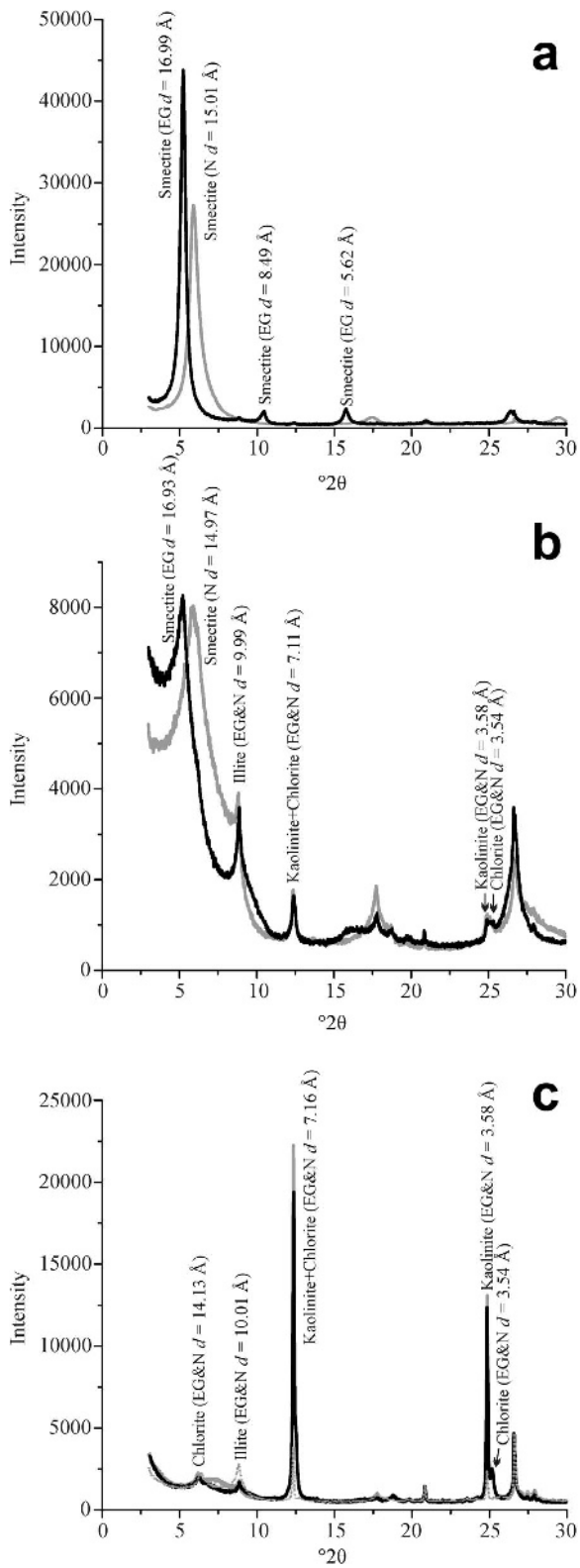

Figure 5. Representative XRD (air-dried (gray), ethylene-glycol solvated (black), and heated (dotted gray)) patterns of <2 μm samples in the SK-1n core. (a) Light gray sandstone sample at 570 m, SK-1n; (b) medium-gray mudstone sample at 800 m, SK-1n; and (c) medium-gray sandstone sample at 1590 m, SK-1n. Abbreviations: N – air-dried, EG – ethylene-glycol solvated, H – heated.

https://doi.org/10.1346/CCMN.2015.0630605 Published online by Cambridge University Press

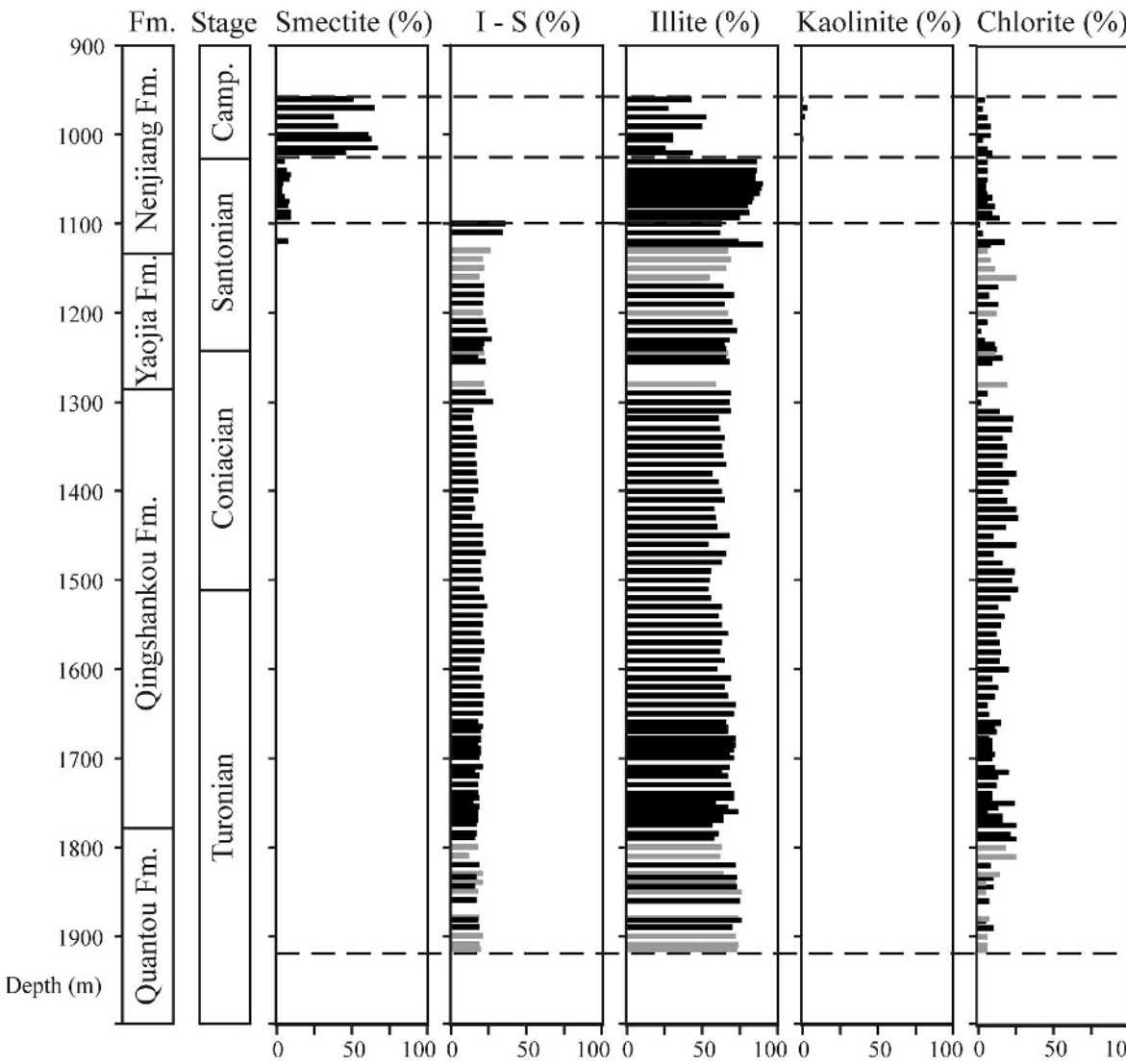

Figure 6. Clay-mineral distribution in the SK-1s core based on XRD results. Black bars – mudstone samples; gray bars – sandstone samples; Camp. – Campanian. Dashed lines separate the intervals with different clay assemblages as described in the text.

al., 2014). This mudstone sample may have experienced a temperature of ~140ºC, although the modern borehole temperature at 1900 m is ~95ºC (Wang, C.S. *et al.*, 2008). Similarly, ~25% smectite in I-S suggests a maximum burial temperature of ~125ºC for the mudstone from 1500 m in SK-1s, compared to a modern borehole temperature of ~75ºC (Wang, C.S. *et al.*, 2008). The transition of smectite to I-S occurs at ~1100 m in SK-1s and, thus, corresponds to a diagenetic temperature of ~100ºC. This estimate agrees with the total organic carbon T_{max} temperature within the oil window (Song *et al.*, 2013; Deconinck *et al.*, 2014). At a depth of 1100 m, the modern borehole temperature was 40–50ºC (Wang, C.S. *et al.*, 2008). The paleogeothermal gradient of the Songliao Basin in the Cretaceous was restored to 4.26–4.80ºC/100 m, based on vitrinite reflectance, inclusion thermometry, and clay-mineral transition temperature (Ren *et al.*, 2001). Assuming that this geothermal gradient has been maintained since the Cretaceous, the erosion of ~1000 m can be inferred since the sediments of SK-1s reached their maximum burial depth. In SK-1n, sediments at 1200–1700 m could reach a maximum paleo-temperature near 100ºC (modern borehole temperature ~50–75ºC, Wang, C.S. *et al.*, 2008), as I-S occurs in this interval. A denudation of ~500–1000 m was, thus, inferred in SK-1n, assuming a similar geothermal gradient of ~5ºC/100 m during the Late Cretaceous.

The tectonic evolution of the Songliao Basin indicates that basin-scale subsidence continued in the Late Cretaceous through the end of deposition of the upper Nenjiang Fm., when the structural inversion and

https://doi.org/10.1346/CCMN.2015.0630605 Published online by Cambridge University Press

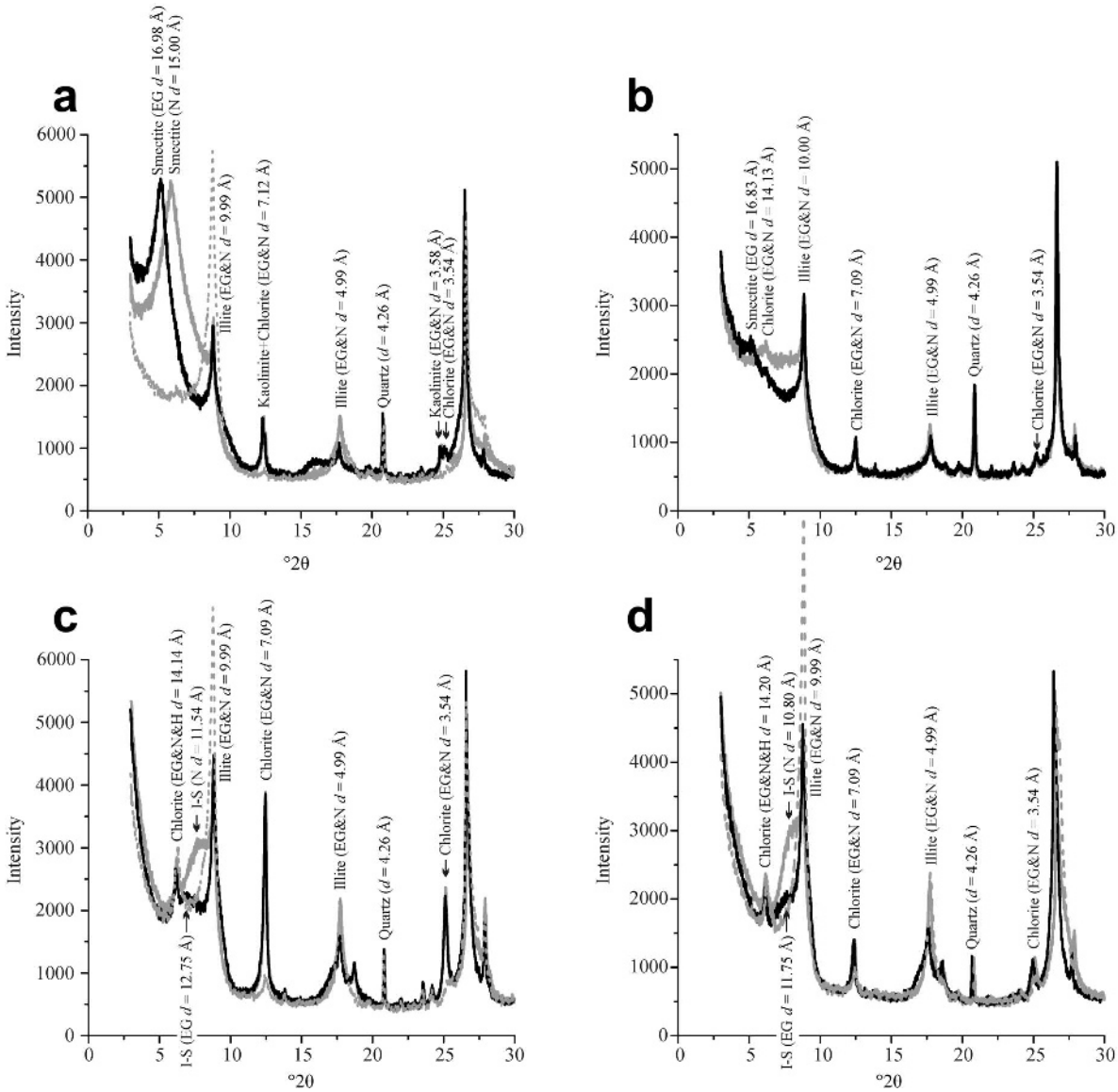

Figure 7. Representative XRD (air-dried (gray), ethylene-glycol solvated (black), and heated (dotted gray)) patterns of <2 μm samples in the SK-1s core. (a) Dark gray mudstone sample at 970 m, SK-1s; (b) grayish black mudstone sample at 1087 m, SK-1s; (c) medium-gray mudstone sample at 1510 m, SK-1s; and (d) grayish-brown silty mudstone at 1915 m, SK-1s. Abbreviations: N – air-dried, EG – ethylene-glycol solvated, H – heated.

denudation started due to the subduction of the Pacific plate (Feng *et al.*, 2010). During the structural inversion stage, two major tectonic events occurred with denudation of sedimentary strata causing two regional unconformities on top of the Nenjiang Fm. and Mingshui Fm., respectively (Chen *et al.*, 2010; Feng *et al.*, 2010). Upon the cessation of deposition of the upper Nenjiang Fm., regional uplift caused denudation of ~500 m in the Central Downwarp Zone (Guo *et al.*, 2009; Chen *et al.*, 2010) in which the SK-1 drilling sites are located (Figure 1). This is consistent with ~400 m of denudation based on a proposed 3.6–4.6 Ma hiatus between the Nenjiang Fm. and the Sifangtai Fm. in SK-1n constrained by biostratigraphy and cyclostratigraphy (Scott *et al.*, 2012; Wu *et al.*, 2015), and assumptions of a continuous sedimentation rate of 183 m/Ma (Deng *et al.*, 2013) for ~2 Ma. Upon cessation of deposition of the Mingshui Fm., strong tectonic movement folded the strata and caused denudation of ~1000 m in the Central Downwarp Zone (Xiang *et al.*, 2007). According to biostratigraphy in the SK-1 cores, the unconformity between the Mingshui Fm. and the overlying Taikang Fm. is estimated to span >30 Ma (Li *et al.*, 2011), much longer than that of the terminal Nenjiang Fm. unconformity. Sediments in both cores probably reached a maximum burial depth and temperature during the

https://doi.org/10.1346/CCMN.2015.0630605 Published online by Cambridge University Press

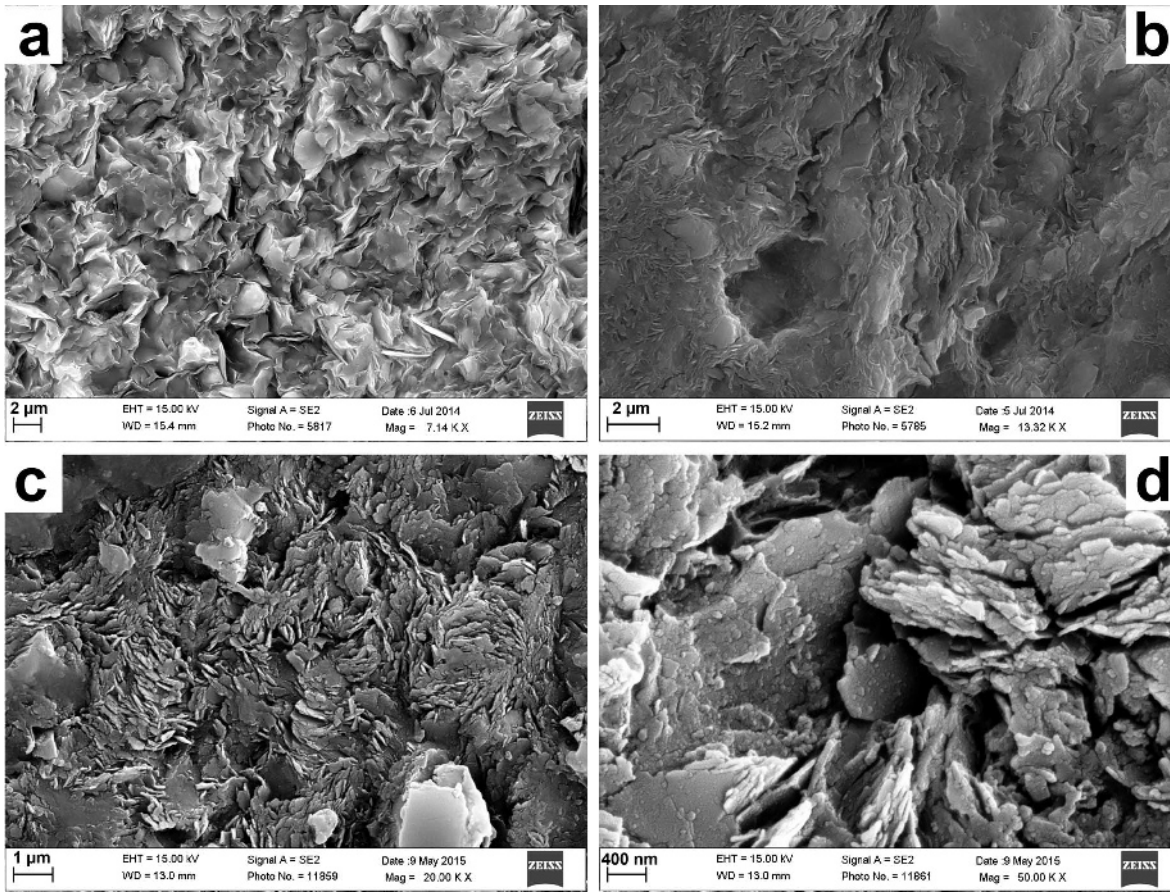

Figure 8. Scanning electron microscopic images of samples in SK-1 cores. (a) Light-gray sandstone sample at 345 m, SK-1n, rose-like smectite; (b) gray mudstone sample at 605 m, SK-1n, platy smectite and illite; (c) medium-gray sandstone sample at 1590 m, SK-1n, stacked plates of kaolinite; and (d) medium-gray sandstone sample at 1590 m, SK-1n, pseudohexagonal outlines of kaolinite.

deposition of the Mingshui Fm. in the latest Cretaceous, and subsequently experienced significant erosion at the end of the Cretaceous and during the Cenozoic. The transition of smectite to I-S in the SK-1 cores and the inferred paleotemperatures and basin denudation history provide new constraints for basin modeling of oil maturation at elevated temperatures in the Songliao Basin.

Early diagenesis of clay minerals in shallow-buried sandstones

Early diagenesis of clay minerals refers to the diagenetic processes influencing shallow-buried sediments, the clay mineral assemblages of which are commonly related to low-temperature fluids but not significantly dependent on the influence of temperature and other factors due to increasing burial depth (Chamley, 1989). Compared with mudstones, clay composition in sandstones may experience obvious early diagenetic modifications because of greater porosity and increased pore fluid (Wilson and Pittman, 1977; Bjørlykke, 1998; Fesharaki *et al.*, 2007).

The fluvial and deltaic sandstones at depths between 1300 m and 1600 m in SK-1n contain a large amount of kaolinite, much more than that of the adjacent mudstones (Figure 4). The kaolinite is characterized by a very sharp 7 Å peak in the XRD pattern in Figure 5c, stacked plates for aggregates, and pseudohexagonal outlines for individual plates under SEM (Figure 8c,d). These features indicate original crystallinity and, thus, an authigenic origin (Wilson and Pittman, 1977; Bjørlykke, 1998).

Authigenic kaolinite usually forms in sandstones from the dissolution or alteration of aluminosilicate minerals such as feldspar aided by the action of low-pH fluid (Bjørlykke, 1998; Khidir and Catuneanu, 2009; Wilson *et al.*, 2014). Feldspar and mica usually provide the Al^{3+} necessary for the formation of kaolinite, while low-pH pore fluids supply the necessary protons and remove the dissolved aqueous species such as Na^{+}, K^{+}, and Si^{4+} (Bjørlykke, 1998; Wilson *et al.*, 2014). The fluid sources of the authigenic kaolinite in SK-1n could be meteoric waters penetrating the sandstones, and/or organic acids derived from the black (oil) shale

https://doi.org/10.1346/CCMN.2015.0630605 Published online by Cambridge University Press

stratigraphically below the kaolinite-rich zone (Figure 3; Wang *et al*., 1990; Bjørlykke, 1998; Wilkinson *et al.*, 2006).

Fluvial sandstones at depths between 300 m and 1200 m in SK-1n are rich in smectite (Figure 4). The high degree of smectite crystallization in the sandstone units is demonstrated by the very large 15 Å peak under air-dried conditions and the 17 Å peak under EG conditions in XRD patterns (Figure 5a). Under SEM analysis, smectite presents 'rose-like' or 'honeycomb' morphology, and forms coatings on detrital grains (Figure 8a; Gao *et al.*, 2013). These features indicate an authigenic origin of smectite (Wilson and Pittman, 1977; Vanderaveroet and Deconinck, 1997; Fesharaki *et al.*, 2007; Gao *et al.*, 2013).

Authigenic smectite is frequently encountered in shallow-buried sandstones, especially when volcaniclastic components are abundant, because neoformation of smectite may be the result of hydrolysis and alteration of primary feldspar and mica (Wilson and Pittman, 1977; Cuadros *et al.*, 1999; Fesharaki *et al.*, 2007; Franke and Ehrmann, 2010). Volcanic lithics previously reported in a shorter interval of the SK-1n core further support an early diagenetic origin for smectite (Gao *et al.*, 2013).

Paleoenvironmental control on clay minerals in shallow-buried mudstones

Clay minerals in the shallow-buried mudstones tend to be more resistant to burial and early diagenetic alterations, when mudstones have low temperature and permeability. These clay minerals are formed under sedimentary conditions, controlled by factors such as provenance, depositional environment, and paleoclimate (Singer, 1984; Thiry, 2000; Sáez *et al.*, 2003; Deconinck *et al.*, 2005; Liu *et al.*, 2010). Consequently, clay assemblages can be used as paleoenvironmental indicators (Deconinck *et al.*, 2000; Dera *et al.*, 2009; Do Campo *et al.*, 2014).

Clay-mineral assemblages in mudstones above ~1200 m in SK-1n are dominated by abundant smectite and illite, minor kaolinite and chlorite, and the absence of I-S, different from the smectite-dominated composition in adjacent sandstones (Figure 4). The platy shapes of these clay minerals indicate a detrital origin (Figure 8b). The temperature reached by the sediments is <<100ºC because such clay minerals tend to be less influenced by thermodynamic effects (as discussed above). Moreover, oscillating depth-dependent variations of smectite and illite are not typical features of burial diagenesis.

The variations of clay mineral assemblages in the 200 m–1200 m interval of SK-1n core (Figure 4) are interpreted as being a result of paleoenvironmental change. Provenance lithology determines the weathering products in the source area which may influence significantly clay assemblages in sedimentary basins (Thiry, 2000; Sáez *et al.*, 2003). During the deposition of the Sifangtai and Mingshui Formations, the provenance was the Lesser Xing'an–Zhangguangcai Range east and north of the Basin (Feng *et al.*, 2010; Wang *et al.*, 2013a). Previous sedimentological and geophysical studies have indicated that these mountain ranges remained tectonically stable during the Late Cretaceous (Feng *et al.*, 2010; Li *et al.*, 2010). The provenance, therefore, changed little and may not be the main control on changes in the clay assemblages observed in the SK-1 core. The depositional environment can influence the clay composition in sedimentary basins during different transportation and deposition processes (Thiry, 2000; Suresh *et al.*, 2004). Clay sorting and differential settling during depositional environment changes, *e.g.* from a trunk to a flood plain, may control frequent changes in clay-mineral assemblages within tens of meters. Such processes, however, could not explain the general trend of increasing smectite and decreasing illite from 1200 m to 200 m as sedimentary facies did not change significantly in this interval (Cheng *et al.*, 2009; Wang *et al.*, 2013a).

Climate may influence the clay-mineral compositions in weathering profiles and soils, in which smectite indicates a seasonally wet-dry climate and illite corresponds to a relatively dry climate (Singer, 1984; Robert and Kennett, 1994; Hong *et al.*, 2007). During the deposition of the Sifangtai and Mingshui Formations, paleosols developed primarily in an alluvial-plain environment (Cheng *et al.*, 2009; Huang *et al.*, 2013; Gao *et al.*, 2015), and could provide a source for clay minerals in the upper strata of the SK-1n core (Gao *et al.*, 2013). The observed trend from an illite-dominated interval (800–1200 m) to a smectite-dominated interval (250–800 m) is, therefore, interpreted as resulting from the transition from a relatively dry climate to a seasonally wet climate. This trend in increasing humidity is consistent with previous paleoclimatic reconstructions in the Songliao Basin. For example, pollen and spores records indicate a semi-arid climate when the Sifangtai Fm. was deposited and a semi-humid climate during deposition of the Mingshui Fm. (Gao *et al.*, 1999; Wang *et al.*, 2013a). Evidence from paleosol types determined by their pedogenic features from these two formations was previously found to indicate a transition to a more humid climate during the latest Cretaceous (Huang *et al.*, 2010; Wang *et al.*, 2013a). Finally, recent stable isotope analyses on pedogenic carbonates from the SK-1n core suggest a general warming and wetting trend over this period (Gao *et al.*, 2015).

CONCLUSIONS

The present study took advantage of the 2500 m of nearly continuous sediments from the Songliao Basin SK-1 cores, and determined the clay mineralogy of the Late Cretaceous terrestrial sediments. Illite is ubiquitous through the succession, smectite is frequently encoun-

https://doi.org/10.1346/CCMN.2015.0630605 Published online by Cambridge University Press

tered in the upper part, and mixed-layer illite-smectite (I-S), chlorite, and kaolinite are abundant in the lower part. The overall trend of decreasing smectite and increasing illite, I-S, and chlorite with increasing depth in both cores was caused largely by burial diagenesis.

Diagenetic clay minerals have been applied in a very limited way to estimate the thermal evolution of sedimentary rocks in previous sedimentology and petroleum-geology studies of the Songliao Basin. Using observations of clay-mineral diagenesis to reconstruct the paleotemperatures and burial depths to which the sediments were subjected, the present study infers that the deeper sediments of the SK-1 cores could have reached a maximum burial depth of ~1000 m deeper than the present-day and temperatures ~50ºC higher than today in the latest Cretaceous. The transition of smectite to I-S in the SK-1 cores and the inferred paleotemperatures provide new constraints for basin modeling of oil maturation at elevated temperatures in the Songliao Basin.

Previous researchers have been cautious about interpreting whether paleoenvironmental proxies in the Songliao Basin were altered by diagenesis. The present study has indicated that authigenic kaolinite and smectite were enriched in sandstones with respect to the coeval mudstones in the SK-1n core as a result of early diagenesis by interaction with primary aluminosilicates and pore fluids. The fluid sources could be meteoric waters penetrating the sandstones, and/or organic acids derived from adjacent dark-colored shale. In the mudstones of the upper strata of the SK-1n core, variations in smectite and illite are primarily controlled by paleoenvironmental changes. In addition, increases in smectite and decreases in illite were observed from the late Campanian to Maastrichtian. Changes in clay mineralogical assemblages indicate the transition from a relatively dry climate to a seasonally wet climate, consistent with previous paleoenvironmental interpretations for the Songliao Basin.

ACKNOWLEDGMENTS

The acting Editor-in-Chief, the associate editor, and three anonymous reviewers are thanked for their helpful comments. The authors thank the staff of the XRD Laboratory, State Key Laboratory of Marine Geology, Tongji University for their advice and assistance during XRD analysis. The authors also thank Dr Dongjie Tang and Dr Wenhao Zhang for their assistance with SEM analysis, and Dr Luba Jansa for helpful discussions. The present study was supported financially by the National Basic Research Program of China (2012CB822000), the Open Fund Project of the State Key Laboratory of Marine Geology, Tongji University (No. MGK1203), and the Fundamental Research Funds for the Central Universities of China (2652015387). Daniel E. Ibarra's participation in the Songliao Basin Continental Scientific Drilling Project was supported by the United States National Science Foundation grant EAR-1423967 to C. Page Chamberlain.

REFERENCES

Bjørlykke, K. (1998) Clay mineral diagenesis in sedimentary basins – a key to the prediction of rock properties. Examples from the North Sea Basin. *Clay Minerals*, **33**, 15–34.

Bjørlykke, K. (2014) Relationships between depositional environments, burial history and rock properties. Some principal aspects of diagenetic process in sedimentary basins. *Sedimentary Geology*, **301**, 1–14.

Chamberlain, C.P., Wan, X., Graham, S.A., Carroll, A.R., Doebbert, A.C., Sageman, B.B., Blisniuk, P., Kent-Corson, M.L., Wang, Z., and Wang, C. (2013) Stable isotopic evidence for climate and basin evolution of the Late Cretaceous Songliao Basin, China. *Palaeogeography, Palaeoclimatology, Palaeoecology*, **385**, 106–124.

Chamley, H. (1989) *Clay Sedimentology*. Springer Verlag, Berlin, 623 pp.

Chen, P. and Chang, Z. (1994) Nonmarine Cretaceous stratigraphy of eastern China. *Cretaceous Research*, **15**, 245–257.

Chen, X., Li, Z.Q., Chen, J.L., Li, H.K., and Zhang, T. (2010) Determination of the reverse period of Songliao Basin, China. *Geological Bulletin of China*, **29**(2/3), 305–311 (in Chinese with English abstract).

Cheng, R., Wang, G., Wang, P., and Gao, Y. (2009) Uppermost Cretaceous sediments: sedimentary microfacies and sedimentary environment evolution of Sifangtai Formation and Mingshui Formation in SK-1(n). *Earth Science Frontiers*, **16**(6), 85–95 (in Chinese with English abstract).

Cuadros, J., Caballero, E., Huertas, F.J., Cisneros, C.J.d., Huertas, F., and Linares, J. (1999) Experimental alteration of volcanic tuff: Smectite formation and effect on ^{18}O isotope composition. *Clays and Clay Minerals*, **47**, 769–776.

Day-Stirrat, R.J., Milliken, K.L., Dutton, S.P., Loucks, R.G., Hillier, S., Aplin, A.C., and Schleicher, A.M. (2010) Open-system chemical behavior in deep Wilcox Group mudstones, Texas Gulf Coast, USA. *Marine and Petroleum Geology*, **27**, 1804–1818.

Deconinck, J.F., Blanc-Valleron, M.M., Rouchy, J.M., Camoin, G., and Badaut-Trauth, D. (2000) Palaeoenvironmental and diagenetic control of the mineralogy of Upper Cretaceous–Lower Tertiary deposits of the Central Palaeo–Andean basin of Bolivia (Potosi area). *Sedimentary Geology*, **132**, 263–278.

Deconinck, J.-F., Amédro, F., Baudin, F., Godet, A., Pellenard, P., Robaszynski, F., and Zimmerlin, I. (2005) Late Cretaceous palaeoenvironments expressed by the clay mineralogy of Cenomanian–Campanian chalks from the east of the Paris Basin. *Cretaceous Research*, **26**, 171–179.

Deconinck, J.F., Crasquin, S., Bruneau, L., Pellenard, P., Baudin, F., and Feng, Q. (2014) Diagenesis of clay minerals and K-bentonites in late Permian/Early Triassic sediments of the Sichuan Basin (Chaotian section, Central China). *Journal of Asian Earth Sciences*, **81**, 28–37.

Deng, C.L., He, H.Y., Pan, Y.X., and Zhu, R.X. (2013) Chronology of the terrestrial Upper Cretaceous in the Songliao Basin, northeast Asia. *Palaeogeography, Palaeoclimatology, Palaeoecology*, **385**, 44–54.

Dera, G., Pellenard, P., Neige, P., Deconinck, J.-F., Pucéat, E., and Dommergues, J.-L. (2009) Distribution of clay minerals in Early Jurassic Peritethyan seas: Palaeoclimatic significance inferred from multiproxy comparisons. *Palaeogeography, Palaeoclimatology, Palaeoecology*, **271**, 39–51.

Do Campo, M., Nieto, F., del Papa, C., and Hongn, F. (2014) Syn- and post-sedimentary controls on clay mineral assemblages in a tectonically active basin, Andean

Argentinean foreland. *Journal of South American Earth Sciences*, **52**, 43–56.

Elliott, W.C. and Matisoff, G. (1996) Evaluation of kinetic models for the smectite to illite transformation. *Clays and Clay Minerals*, **44**, 77–87.

Fesharaki, O., García-Romero, E., Cuevas-González, J., and López-Martínez, N. (2007) Clay mineral genesis and chemical evolution in the Miocene sediments of Somosaguas, Madrid Basin, Spain. *Clay Minerals*, **42**, 187–201.

Feng, Z.Q., Jia, C.Z., Xie, X.N., Zhang, S., Feng, Z.H., and Cross, T.A. (2010) Tectonostratigraphic units and stratigraphic sequences of the nonmarine Songliao Basin, northeast China. *Basin Research*, **22**, 79–95.

Feng, Z., Wang, C., Graham, S., Koeberl, C., Dong, H., Huang, Y., and Gao, Y. (2013) Continental scientific drilling project of Cretaceous Songliao Basin: Scientific objectives and drilling technology. *Palaeogeography, Palaeoclimatology, Palaeoecology*, **385**, 6–16.

Franke, D. and Ehrmann, W. (2010) Neogene clay mineral assemblages in the AND-2A drill core (McMurdo Sound, Antarctica) and their implications for environmental change. *Palaeogeography, Palaeoclimatology, Palaeoecology*, **286**, 55–65.

Fu, M., Zhang, S., Ding, X., Liao, Q., Xiong, D., and Zhu, Z. (2012) Characteristics and petroleum geologic significances of clay rims in sandstones of Mingshui Formation, well Songke 1, Songliao Basin. *Petroleum Geology and Experiment*, **34**, 587–592 (in Chinese with English abstract).

Gao, R.Q., Zhao, C.B., Qiao, X.Y., Zheng, Y.L., Yan, F.Y., and Wan, C.B. (1999) *Cretaceous Oil Strata Palynology from Songliao Basin*. Geological Publishing House, Beijing (in Chinese).

Gao, Y., Wang, C., Liu, Z., Zhao, B., and Zhang, X. (2013) Clay mineralogy of the middle Mingshui Formation (upper Campanian to lower Maastrichtian) from the SK-1n borehole in the Songliao Basin, NE China: Implications for palaeoclimate and provenance. *Palaeogeography, Palaeoclimatology, Palaeoecology*, **385**, 162–170.

Gao, Y., Ibarra, D.E., Wang, C., Caves, J.K., Chamberlain, C.P., Graham, S.A., and Wu, H. (2015) Mid-latitude terrestrial climate of East Asia linked to global climate in the Late Cretaceous. *Geology*, **43**, 287–290.

Graham, S.A., Hendrix, M.S., Johnson, C.L., Badamgarav, D., Badarch, G., Amory, J., Porter, M., Barsbold, R., Webb, L.E., and Hacker, B.R. (2001) Sedimentary record and tectonic implications of Mesozoic rifting in southeast Mongolia. *Geological Society of America Bulletin*, **113**, 1560–1579.

Guo, W., Yu, W., Liu, Z., and Ma, L. (2009) The burial history of the southern Songliao Basin. *Journal of Jilin University (Earth Science Edition)*, **39**, 353–360 (in Chinese with English abstract).

He, H., Deng, C., Wang, P., Pan, Y., and Zhu, R. (2012) Toward age determination of the termination of the Cretaceous Normal Superchron. *Geochemistry, Geophysics, Geosystems*, **13**, Q02002.

Hong, H., Li, Z., Xue, H., Zhu, Y., Zhang, K., and Xiang, S. (2007) Oligocene clay mineralogy of the Linxia Basin: Evidence of paleoclimatic evolution subsequent to the initial-stage uplift of the Tibetan Plateau. *Clays and Clay Minerals*, **55**, 491–503.

Hou, Q.J., Feng, Z.Q., and Feng, Z.H. (2009) *Terrestrial Petroleum Geology of Songliao Basin*. Petroleum Industry Press, Beijing (in Chinese).

Hower, J., Eslinger, E.V., Hower, M.E., and Perry, E.A. (1976) Mechanism of burial metamorphism of argillaceous sediment: 1. Mineralogical and chemical evidence. *Geological Society of America Bulletin*, **87**, 725–737.

Huang, C., Retallack, G.J., and Wang, C. (2010) Cretaceous calcareous paleosols: pedogenetic characteristics and paleoenvironmental implications. *Acta Pedologica Sinica*, **47**, 1029–1038.

Huang, C., Retallack, G.J., Wang, C., and Huang, Q. (2013) Paleoatmospheric pCO_2 fluctuations across the Cretaceous–Tertiary boundary recorded from paleosol carbonates in NE China. *Palaeogeography, Palaeoclimatology, Palaeoecology*, **385**, 95–105.

Huang, W.-L., Longo, J.M., and Pevear, D.R. (1993) An experimentally derived kinetic model for smectite-to-illite conversion and its use as a geothermometer. *Clays and Clay Minerals*, **41**, 162–177.

Khidir, A. and Catuneanu, O. (2009) Basin-scale distribution of authigenic clay minerals in the late Maastrichtian–early Paleocene fluvial strata of the Alberta foredeep: Implications for burial depth. *Bulletin of Canadian Petroleum Geology*, **57**, 251–274.

Li, J., Batten, D.J., and Zhang, Y. (2011) Palynological record from a composite core through Late Cretaceous–Early Paleocene deposits in the Songliao Basin, northeast China and its biostratigraphic implications. *Cretaceous Research*, **32**, 1–12.

Liu, Y. (1985) Clay minerals of Late Cretaceous Songliao Basin and their sedimentary environment. *Acta Sedimentologica Sinica*, **3**, 131–139 (in Chinese with English abstract).

Liu, Z., Colin, C., Trentesaux, A., Blamart, D., Bassinot, F., Siani, G., and Sicre, M.A. (2004) Erosional history of the eastern Tibetan Plateau since 190 kyr ago: clay mineralogical and geochemical investigations from the southwestern South China Sea. *Marine Geology*, **209**, 1–18.

Liu, Z., Colin, C., Li, X., Zhao, Y., Tuo, S., Chen, Z., Siringan, F.P., Liu, J.T., Huang, C.-Y., You, C.-F., and Huang, K.-F. (2010) Clay mineral distribution in surface sediments of the northeastern South China Sea and surrounding fluvial drainage basins: Source and transport. *Marine Geology*, **277**, 48–60.

Moore, D.M. and Reynolds, R.C. (1997) *X-ray Diffraction and the Identification and Analysis of Clay Minerals*, 2nd edition. Oxford University Press Inc., New York.

Osborn, S.G., Duffield, L.T., Elliott, W.C., Wampler, J.M., Elmore, R.D., and Engel, M.H. (2014) The timing of diagenesis and thermal maturation of the Cretaceous Marias River shale, Disturbed Belt, Montana. *Clays and Clay Minerals*, **62**, 112–125.

Peltonen, C., Marcussen, Ø., Bjørlykke, K., and Jahren, J. (2009) Clay mineral diagenesis and quartz cementation in mudstones: The effects of smectite to illite reaction on rock properties. *Marine and Petroleum Geology*, **26**, 887–898.

Petschick, R., Kuhn, G., and Gingele, F. (1996) Clay mineral distribution in surface sediments of the South Atlantic: sources, transport, and relation to oceanography. *Marine Geology*, **130**, 203–229.

Pytte, A. and Reynolds, R.C. (1988) The thermal transformation of smectite to illite. Pp. 133–140 in: *Thermal History of Sedimentary Basins* (N.D. Naeser and T.H. McCulloh, editors). Springer-Verlag, Berlin.

Ren, J., Tamaki, K., Li, S., and Junxia, Z. (2002) Late Mesozoic and Cenozoic rifting and its dynamic setting in eastern China and adjacent areas. *Tectonophysics*, **344**, 175–205.

Ren, Z., Xiao, D., and Chi, Y. (2001) Restoration of the palaeogeotherm in Songliao Basin. *Petroleum Geology and Oilfield Development in Daqing*, **20**, 13–14 (in Chinese with English abstract).

Robert, C. and Kennett, J.P. (1994) Antarctic subtropical humid episode at the Paleocene–Eocene boundary: Clay-mineral evidence. *Geology*, **22**, 211–214.

Sáez, A., Inglès, M., Cabrera, L., and de las Heras, A. (2003) Tectonic–palaeoenvironmental forcing of clay-mineral assemblages in nonmarine settings: The Oligocene–Miocene As Pontes Basin (Spain). *Sedimentary Geology*, **159**, 305–324.

Scott, R.W., Wan, X., Wang, C., and Huang, Q. (2012) Late Cretaceous chronostratigraphy (Turonian–Maastrichtian): Sk1 core Songliao Basin, China. *Geoscience Frontiers*, **3**, 357–367.

Singer, A. (1984) The paleoclimatic interpretation of clay minerals in sediments – a review. *Earth-Science Reviews*, **21**, 251–293.

Song, Z., Qin, Y., George, S.C., Wang, L., Guo, J., and Feng, Z. (2013) A biomarker study of depositional paleoenvironments and source inputs for the massive formation of Upper Cretaceous lacustrine source rocks in the Songliao Basin, China. *Palaeogeography, Palaeoclimatology, Palaeoecology*, **385**, 137–151.

Środoń, J. (1999) Nature of mixed-layer clays and mechanisms of their formation and alteration. *Annual Review of Earth and Planetary Sciences*, **27**, 19–53.

Środoń, J., Clauer, N., Huff, W., Dudek, T., and Banaś, M. (2009) K-Ar dating of the lower Palaeozoic K-bentonites from the Baltic Basin and the Baltic Shield: Implications for the role of temperature and time in the illitization of smectite. *Clay Minerals*, **44**, 361–387.

Środoń, J., Paszkowski, M., Drygant, D., Anczkiewicz, A., and Banaś, M. (2013) Thermal history of Lower Paleozoic rocks on the peri-Tornquist margin of the east European craton (Podolia, Ukraine) inferred from combined XRD, K-Ar, and ATF data. *Clays and Clay Minerals*, **61**, 107–17732.

Sun, S., Shu, L., Zeng, Y., Cao, J., and Feng, Z. (2007) Porosity–permeability and textural heterogeneity of reservoir sandstones from the lower Cretaceous Putaohua Member of Yaojia Formation, Weixing Oilfield, Songliao Basin, northeast China. *Marine and Petroleum Geology*, **24**, 109–127.

Suresh, N., Ghosh, S.K., Kumar, R., and Sangode, S. (2004) Clay-mineral distribution patterns in late Neogene fluvial sediments of the Subathu sub-basin, central sector of Himalayan foreland basin: Implications for provenance and climate. *Sedimentary Geology*, **163**, 265–278.

Thiry, M. (2000) Palaeoclimatic interpretation of clay minerals in marine deposits: An outlook from the continental origin. *Earth-Science Reviews*, **49**, 201–221.

Vanderaveroet, P. and Deconinck, J.F. (1997) Clay mineralogy of Cenozoic sediments of the Atlantic city Borehole, New Jersey. *Proceedings of the Ocean Drilling Program, Scientific Results*, **150 X**, 49–57.

Velde, B. and Vasseur, G. (1992) Estimation of the diagenetic smectite-to-illite transformation in time-temperature space. *American Mineralogist*, **77**, 967–976.

Wan, X., Zhao, J., Scott, R.W., Wang, P., Feng, Z., Huang, Q., and Xi, D. (2013) Late Cretaceous stratigraphy, Songliao Basin, NE China: Sk1 cores. *Palaeogeography, Palaeoclimatology, Palaeoecology*, **385**, 31–43.

Wang, C.S., Feng, Z.Q., Wu, H.Y., Wang, P.J., Feng, Z.H., and Ren, Y.G. (2008) Preliminary achievement of the Chinese Cretaceous Continental Scientific Drilling Project – SK-I. *Acta Geologica Sinica*, **82**, 9–20 (in Chinese with English abstracts).

Wang, C., Feng, Z., Zhang, L., Huang, Y., Cao, K., Wang, P., and Zhao, B. (2013a) Cretaceous paleogeography and paleoclimate and the setting of SKI borehole sites in Songliao basin, northeast China. *Palaeogeography, Palaeoclimatology, Palaeoecology*, **385**, 17–30.

Wang, C., Scott, R.W., Wan, X., Graham, S.A., Huang, Y., Wang, P., Wu, H., Dean, W.E., and Zhang, L. (2013b) Late Cretaceous climate changes recorded in Eastern Asian lacustrine deposits and North American Epieric Sea strata. *Earth-Science Reviews*, **126**, 275–299.

Wang, D.P., Liu, Z.J., and Liu, L. (1994) *Evolution of Songliao Basin and Fluctuation of the Sealevel*. Geological Publishing House, Beijing (in Chinese).

Wang, G., Cheng, R., Wang, P., and Gao, Y. (2008) The forming mechanism of dolostone of Nengjiang Formation in Songliao Basin – Example from CCSD-SK. *Acta Geologica Sinica*, **82**(2), 48–54 (in Chinese with English abstract).

Wang, X., Xin, G., and Feng, Y. (1990) *Study on clay mineralogy of the Songliao Basin*. Heilongjiang Science and Technology Press, Harbin, China (in Chinese).

Wilkinson, M., Haszeldine, R.S., and Fallick, A.E. (2006) Jurassic and Cretaceous clays of the northern and central North Sea hydrocarbon reservoirs reviewed. *Clay Minerals*, **41**, 151–186.

Wilson, M.D. and Pittman, E.D. (1977) Authigenic clays in sandstones; recognition and influence on reservoir properties and paleoenvironmental analysis. *Journal of Sedimentary Research*, **47**, 3–31.

Wilson, M.J., Wilson, L., and Patey, I. (2014) The influence of individual clay minerals on formation damage of reservoir sandstones: A critical review with some new insights. *Clay Minerals*, **49**, 147–164.

Wu, H., Zhang, S., Jiang, G., Hinnov, L., Yang, T., Li, H., Wan, X., and Wang, C. (2013) Astrochronology of the early Turonian–early Campanian terrestrial succession in the Songliao Basin, northeastern China and its implication for long-period behavior of the solar system. *Palaeogeography, Palaeoclimatology, Palaeoecology*, **385**, 55–70.

Wu, H.C., Zhang, S.H., Hinnov, L.A., Jiang, G.Q., Yang, T.S., Li, H.Y., Wan, X.Q., and Wang, C.S. (2015) Cyclostratigraphy and orbital tuning of the terrestrial upper Santonian–Lower Danian in Songliao Basin, northeastern China. *Earth and Planetary Science Letters*, **407**, 82–95.

Xiang, C., Feng, Z., Pang, X., Wu, H., and Li, J. (2007) Late stage thermal history of the Songliao Basin and its tectonic implications: Evidence from apatite fission track (AFT) analyses. *Science in China Series D: Earth Sciences*, **50**, 1479–1487.

(*Received 26 November 2014; revised 20 December 2015; Ms. 934; AE: H. Dong*)